First record of carbonates with spherulites and cone-in-cone structures from the Precambrian of Arctic Norway, and their palaeoenvironmental significance

Guido Meinhold[1,2,*], Sören Jensen[3], Magne Høyberget[4], Arzu Arslan[5], Jan Ove R. Ebbestad[6], Anette E. S. Högström[7], Teodoro Palacios[3], Heda Agić[8], Wendy L. Taylor[9]

[1]*School of Geography, Geology and the Environment, Keele University, Keele, ST5 5BG, UK*

[2]*Department of Sedimentology and Environmental Geology, University of Göttingen, Goldschmidtstraße 3, D-37077 Göttingen, Germany*

[3]*Área de Paleontología, Facultad de Ciencias, Universidad de Extremadura, Avenida de Física, E-06006 Badajoz, Spain*

[4]*Rennesveien 14, N-4513 Mandal, Norway*

[5]*Newcastle-under-Lyme, Staffordshire, ST5 2ND, UK*

[6]*Museum of Evolution, Uppsala University, Norbyvägen 16, SE 752 36 Uppsala, Sweden*

[7]*Arctic University Museum of Norway, UiT - The Arctic University of Norway, N-9037 Tromsø, Norway*

[8]*Department of Earth Science, University of California at Santa Barbara, Santa Barbara, CA 93106, USA*

[9]*Department of Geological Sciences, University of Cape Town, Private Bag X3, Rondebosch 7701, Republic of South Africa*

*Corresponding author.

E-mail address: g.meinhold@keele.ac.uk (G. Meinhold).

Abstract

We report for the first time carbonates from the upper Ediacaran sedimentary succession of Finnmark, Arctic Norway. Carbonates occur as calcareous siliciclastic beds, lenses, and concretions, some with calcite spherulites and cone-in-cone (CIC) calcite, in a mudrock to fine-grained sandstone succession from approximately 3 m to 26 m above the base of the 2nd cycle of the Manndrapselva Member of the Stáhpogieddi Formation (Vestertana Group). They occur *c.* 40 m below the Ediacaran–Cambrian boundary, which is well defined by trace fossils. Thin-section petrography and scanning micro X-ray fluorescence elemental mapping reveal a layered composition of the calcareous sedimentary rocks. In some of those, well-developed nested cones of CIC calcite form the outer layer. Thin clay coatings outline individual cones. The inner layers are composed of (1) carbonate with calcite spherulites (grainstone) and (2) thinly laminated fine-grained calcareous siliciclastics (mudstone and wackestone) indicated by elevated concentrations of Al, Si, Fe, and Ti. The inner siliciclastic layers contain framboidal pyrite and probably organic matter. Formation of calcite spherulites took place probably at the sediment–water interface either in a coastal littoral environment or in situ in the sublittoral zone under high alkaline conditions whereas CIC calcite formed during burial diagenesis and clearly in pre-Caledonian time before metamorphism and cleavage formation. This new record of carbonates with calcite spherulites and CIC structures from the Ediacaran of Arctic Norway adds to their rare occurrences in the geological record.

Keywords: carbonates; calcite spherulites; cone-in-cone structures; Ediacaran; Norway; Baltica.

1. Introduction

The remote Digermulen Peninsula of the Tanafjorden area in eastern Finnmark, Arctic Norway (Fig. 1), has attracted renewed research interest because of new findings of Ediacaran-aged fossils (e.g., Högström et al., 2013, 2014, 2017; Jensen et al., 2018a, 2018b). To date, it has been thought that the entire upper Ediacaran and Cambrian succession of the area comprises only siliciclastic sedimentary rocks. However, this is not the case, and we describe for the first time the carbonates from this succession (Figs. 1 and 2).

Among the sedimentary rocks, carbonates are often used to reconstruct the ocean redox evolution, perturbations in the carbon cycle, and their relationship with biotic changes owing to its well-preserved fossils, and shelf-basin sedimentary sections. The most common type among carbonate rocks are homogeneous calcareous beds made up of chemically precipitated carbonate minerals (mainly calcite which is the most stable polymorph of $CaCO_3$) and/or calcareous fossils (e.g., mollusc shells, coral skeletons, coccolithophores). With the exception of the Lower Cretaceous lacustrine carbonate reservoirs in the South

Atlantic from offshore Brazil (Terra et al., 2010; Wright and Barnett, 2015; Herlinger et al., 2017) and offshore Angola (Saller et al., 2016), less common in the sedimentary record but of great interest for sedimentologists are carbonates made up of calcareous spherulites (Fig. 3).

Carbonate spherulites are spherical to ellipsoidal polycrystalline structures of commonly calcite displaying a fibro-radial texture (Chafetz and Butler, 1980; Verrecchia et al., 1995), and structurally different from ooids (Fig. 3). Carbonate spherulites can form in various depositional environments, ranging from continental (e.g., hot spring, lacustrine, sabkha settings) to marine (Allen, 1936; Hodgson, 1968; Verrecchia et al., 1995; McBride et al., 2003; Mercedes-Martín et al., 2017; Rogerson et al., 2017; Chafetz et al., 2018; Kirkham and Tucker, 2018). Their formation is often related to microbial activity (e.g., the occurrence of extracellular polymeric substances), which generated a favourable microenvironment for calcium carbonate precipitation, at the sediment–water interface or a few cm to m below the interface (e.g., Buczynski and Chafetz, 1991; Verrecchia et al., 1995; Mercedes-Martín et al., 2016; Kirkham and Tucker, 2018); however, an abiotic origin has also been suggested (e.g., Wright and Barnett, 2015). Calcite forming spherulites is suggested to be either replaced aragonite, vaterite, or original (e.g., Tucker, 2001; Wright and Barrett, 2015). Unlike botryoidal morphologies (Grotzinger and Kasting, 1993; Riding, 2008), carbonate spherulites are rare in the Precambrian sedimentary rock record. Carbonate spherulites were described from, for example, the Neoproterozoic Biri Formation of the Hedmark Group of southern Norway (Tucker, 1983) and the Limestone–Dolomite 'Series' of the Eleonore Bay Supergroup of central East Greenland (Fairchild, 1991). Similar forms were also described from the Mesoproterozoic Huanglianduo Formation (Xiao et al., 1997) and Gaoyuzhuang Formation (Seong-Joo and Golubic, 1999) of China.

Cone-in-cone (CIC) structures are another rare feature in carbonate rocks. They are usually made of calcite consisting of multiple nested circular cones forming more or less densely packed sets of columns (e.g., Usdowski, 1963; Woodland, 1964; Franks, 1969; Cobbold and Rodriguez, 2007; Kowal-Linka, 2010) (Fig. 3). They occur commonly in association with concretions and calcareous lenses, or in bedding parallel veins originating from calcareous sedimentary rocks (Usdowski, 1963; Hodgson, 1968; Franks, 1969; Raiswell, 1971; Sellés-Martínez, 1996; Cobbold and Rodriguez, 2007; Kowal-Linka, 2010). CIC calcite is common in organic-rich calcareous mudstone of marine origin (Cobbold et al., 2013).

Their formation has been subject to considerable discussion (e.g., Tarr, 1932; Usdowski, 1963; Franks, 1969; Pettijohn, 1975; Sellés-Martínez, 1994; Kolokol'tsev, 2002; Cobbold and Rodriguez, 2007; Kowal-Linka, 2010; Hooker and Cartwright, 2016; Kershaw and Guo, 2016; Cao et al., 2017). Today, it is generally accepted that CIC calcite forms by precipitation, mainly from supersaturated aqueous solutions, as a result of chemical reactions, or changes in physical conditions, especially temperature and pressure, in bedding parallel fractures that formed by fluid overpressure or by force of crystallization (Cobbold and Rodriguez, 2007; Cobbold et al., 2013, and references therein). Hooker and Cartwright (2016) presented evidence that CIC in general does not form over multiple stages and mineral aggregates composing the structure precipitate with their conical form displacing host sediment. CIC structures have been found worldwide in Phanerozoic sedimentary rocks; however, they are rare in the Precambrian rock record (Cobbold et al., 2013). From the Precambrian, so far CIC calcite has been described from the Palaeoproterozoic of North America (Turner and Kamber, 2012), the Mesoproterozoic of Scotland (Parnell et al., 2014), the lower Ediacaran of the southern Canadian Cordillera (Smith, 2009), and the upper Ediacaran of Ukraine and Moldavia (Văscăutanu, 1931; Kopeliovich, 1965; Ivantsov et al., 2015; Nesterovsky et al., 2017).

In this study, we describe for the first time carbonates, some with calcite spherulites and CIC structures, from the upper Ediacaran of Finnmark, Arctic Norway. The present paper aims to assess the sedimentary and post-sedimentary processes leading to the formation of these types of carbonates and structures. The results of this study may be of interest for sedimentologists working on palaeoenvironmental reconstructions at the Ediacaran–Cambrian transition. They may also be of interest for geobiologists, as carbonate formation, especially in the case of calcite spherulites, is commonly thought to be closely associated with microbial activity (e.g., Buczynski and Chafetz, 1991; Verrecchia et al., 1995; Mercedes-Martín et al., 2016; Kirkham and Tucker, 2018), although non-microbial processes cannot be ruled out (Wright and Barnett, 2015).

2. Geological setting

The study area is located in eastern Finnmark, Arctic Norway (Fig. 1a). Here a ~2.9 km thick succession of Cryogenian to lowermost Ordovician dominantly siliciclastic sedimentary rocks

(Vestertana and Digermulen groups) is preserved within the Gaissa Nappe Complex and parautochthonous in the Tanafjorden–Varangerfjorden region (Reading, 1965; Banks et al., 1971; Rice, 2014) (Fig. 1a), located to the south of the Trollfjorden–Komagelva Fault Zone (Fig. 1a), along which a maximum of about 200 km of dextral displacement is estimated (Rice, 2014). The Vestertana and Digermulen groups are well exposed on the Digermulen Peninsula (Fig. 1a). The Stáhpogieddi Formation of the Vestertana Group has received much attention in recent years as it contains the only Ediacara-type fossils in Scandinavia as well as its most complete Ediacaran–Cambrian transition (Farmer et al., 1992; Högström et al. 2013, 2014, 2017; Jensen et al., 2018a, 2018b) (Fig. 1b). The Stáhpogieddi Formation comprises siliciclastic sedimentary rocks deposited mainly in a marine environment (Reading, 1965; Banks et al., 1971). The highest member in the Stáhpogieddi Formation, the Manndrapselva Member, consists of a basal sandstone-dominated part and two upwards-coarsening cycles. Based on trace fossils, palaeopascichnids, and organic-walled microfossils, the Ediacaran–Cambrian boundary is close to the base of the 3rd cycle of the Manndrapselva Member (Högström et al., 2013; McIlroy and Brasier, 2017; Jensen et al., 2017, 2018a, 2018b) (Fig. 1c).

Of special interest in this study is the 2nd cycle of the Manndrapselva Member which has a total thickness of ~60 m and is well exposed along a coastal section at the eastern part of the Digermulen Peninsula (geographic coordinates: 70°35.517’N, 28°11.505’E) (Fig. 1a–c). The succession comprises alternating thin layers of silt- and mudstone and minor sandstone (Fig. 2). Some of the sandstone beds show wave-formed ripple marks. The siltstone and sandstone layers become gradually thicker towards a prominent sandstone bed higher up in the section, but commonly not exceeding 15 cm in thickness. Flute casts in the lower part of the succession indicate palaeocurrent flow from the N/NE (Fig. 2). The rocks show cleavage, particularly well developed in the muddy sediments. Trace fossils appear in the lower 1–2 m (occasionally up to 4 m) of the section, then they are absent – probably due to a combination of less favourable outcrop and more erosive event beds – until the 24–25 m level where trace fossils again show up (Fig. 2). The trace fossil assemblage of the Manndrapselva Member attests to its marine nature, and the sedimentology is consistent with deposition in a wave-dominated delta or shoreface (McIlroy and Brasier, 2017). Each of the three Manndrapselva Member cycles represents a regressive parasequence (Banks et al., 1971; McIlroy and Brasier, 2017).

During recent fieldwork, we made the first discovery of carbonates within the 2nd cycle of the Manndrapselva Member. The carbonates occur as beds, lenses and concretions. Some show cone-in-cone (CIC) structures and were recovered for follow-up laboratory analysis.

The upper Ediacaran succession was deposited along the western margin of Baltica (in present-day coordinates) in a marine basinal environment (Fig. 1d). The rocks were metamorphosed during the Scandinavian Caledonian orogeny (Meinhold et al., in press).

3. Methodology

Bedrock sample material was cut with a rock saw perpendicular to the bedding to obtain rock slices for thin-section preparation and chemical elemental mapping. Petrographic examination was done with a polarizing light microscope. Chemical elemental mapping was done with a M4 Tornado micro X-ray fluorescence (μ-XRF) spectrometer from Bruker. Conditions included an accelerating voltage of 50 kV and a current of 400 μA with 10 ms per pixel spectrum acquisition and a pixel step-size of 30 μm. Backscattered electron imaging was done by scanning electron microscopy (SEM) with a TM3000 Tabletop Microscope (Benchtop SEM) from Hitachi. The same instrument equipped with an energy dispersive X-ray spectrometer (EDX) was used for single spot chemical analysis. Conditions included an accelerating voltage of 15 kV and a beam diameter of 10 μm.

4. Results

We describe carbonates from the upper Ediacaran of northern Norway for the first time (Figs. 1–9). They occur in a silt- and mudstone-dominated succession from approximately 3 m to 26 m above the base of the 2nd cycle of the Manndrapselva Member of the Stáhpogieddi Formation (Figs. 1b and 2).

The carbonates form laterally discontinuous beds, lenses, and concretions up to 15 cm thick (Fig. 4a–c), randomly distributed through the section. The calcareous concretions are ellipsoidal and their thickness is less than half of their length (Figs. 4 and 5).

Some concretions contain calcite veins and cracks showing tip splays, which are at a high-angle to the bedding (Figs. 4b and 5c). They are slightly curved, localized inside the concretions and do not cut through or reach the concretion rims. A northwest-dipping pervasive cleavage cuts the bedding (Figs. 4b, d and 5c, d).

Already visual observation of hand specimens reveals a layered subdivision of concretions with CIC structures forming the outer layer, with carbonate spherulites and often thinly laminated calcareous siliciclastics forming the inner layers (Figs. 4e and 6).

4.1. Cone-in-cone structures

CIC structures (Figs. 3, 4 and 5) are often found aligned on both sides of calcareous lenses and around calcareous concretions which are mainly made up of carbonate spherulites. They are also observed occasionally along the calcareous siliciclastic beds within the succession (Fig. 4c, d). Cones are usually arranged with their axes perpendicular to the concretion rim and bedding, and are about 1 cm high. The apices of cones point towards the concretions, and their bases are parallel to the bedding interface with the mudstones (Fig. 4d–f). On bedding planes characteristic features are visible (Fig. 5a, b). On less weathered outer surfaces of calcareous lenses and concretions (i.e., in sections normal to the cone axis), they look like circular densely packed blobs (Fig. 5a) or circles made up of overlapping multiple small arcs (Fig. 5b). Nested cones are visible as concentric rings (Fig. 5a, b). Their diameters range from mm to cm scale, not exceeding 2 cm. On intensely weathered surfaces, missing cone cups create empty conic holes with cone apices pointing towards the centre of the calcareous concretions (Fig. 5a).

In sections normal to the bedding, the conic geometry of CIC structures is well observed (Figs. 4d–f, 5c, d and 6). However, an ellipsoidal to sigmoidal geometry is also observed where the cone geometry was modified by later deformation (Figs. 4b, 5d and 6a, c, e), probably during the Scandinavian Caledonian orogeny. The long axes of these ellipsoidal structures lie at about 30° to 40° to the bedding.

In thin sections, CIC structures show dense packing (Fig. 7a, b). The neighbouring cones look overlapping and stepping sideways. The main larger cones are made up of small cones attached to them, also called conical scales (Sellés-Martínez, 1994) (Fig. 7a, b). Although some of the large cones look slightly blunted around their tip region, the attached smaller cones inside the main cones preserve their sharp angular geometry. The cone axes are normal to the bedding. The apical angles of the cones usually range from about 30° to 80° where it could be measured in parts less affected by later deformation. The cones have irregularly corrugated sides from smooth wavy to stepped which are often lined by a thin film of clay minerals. The cones are made up of calcite and enclose only very minor small quartz grains. The cleavage cuts the CIC structures at a small angle. The cones along the upper rim of the concretions were often more severely affected by deformation (Fig. 7c, d) than those along the lower rim.

4.2. Carbonate spherulites

Carbonate spherulite layers (grainstones, according to the classification system for carbonate sedimentary rocks of Dunham, 1962) are found alternating with the thinly laminated calcareous siliciclastic layers (Figs. 6 and 8a, b). The carbonate spherulites are made up of calcite. They are commonly 1 to 3 mm in diameter with greatest abundance around 2 mm, where more or less complete ones could be measured. The spheroidal shape is clearly visible despite partial dissolution (Fig. 8a–e). The individual grains have a radial structure (Fig. 3), consisting of radial calcite fibres that extend from the centre of the grains outward towards the spherulite rim in a fan-like pattern. Well-developed uniaxial-cross extinction pattern shows a set of four symmetric sectors of extinction, also known as Maltese cross extinction pattern, visible under crossed nicols (Fig. 8b, c). Some of the spherulites present one or two concentric rings visible close to their centre or outer rim (Fig. 8d, e).

The dissolution is localized along the contact zones between the spherulites which led to pressure solution seams and stylolites lying at a low to moderate angle to the bedding (Fig. 8a–e). The pressure solution seams are made up of insoluble material, mainly clay minerals. They show an anastomosing pattern. Fibrous calcite crystallized alongside the calcite spherulites in small gashes; the latter are oriented at a high angle to the bedding (Fig. 8d, e). The newly grown calcite fibres are bright white on the photomicrographs. The insoluble material is also present alongside the newly grown fibrous calcite along the spherulite rims. In thin section, it looks like the calcite fibres are dominant on one side of the spherulites (Fig. 8d), although fibre growth on both sides is also present (Fig. 8e).

The thinly laminated calcareous siliciclastic layers alternating with the spherulite layers inside the concretion, which have a composition similar to the individual calcareous beds in the succession, are composed of mainly angular quartz grains floating in a calcite matrix (Fig. 8a, b). Quartz grain size is smaller on average than that of the individual calcareous beds. The amount of quartz grains is about 7% and calcite 93%. There are also small aggregates of framboidal pyrite (Fig. 8f), 6 to 15 µm in diameter with greatest abundance around 10 µm. The size of individual pyrite cubes is about 1 µm on average.

Chemical element mapping reveals a more detailed view on the layered subdivision (Fig. 6e, f). The cones are horizontally closely packed, made of calcite (molar Mg/Ca ratios of 0.02–0.03) with thin clay coatings outlining individual cones, as evidenced by elevated concentrations of Al, Si, K, Ti, and Fe (Appendix A). Both the middle and inner layers seem to contain organic matter as suggested by elevated concentrations of sulphur.

4.3. Calcareous siliciclastic beds

The calcareous siliciclastic beds are made up of mainly angular quartz grains floating in a calcite matrix (mudstone and wackestone, according to the classification system for carbonate sedimentary rocks of Dunham, 1962) (Fig. 7e, f). Quartz grains are well sorted, and usually less than 100 µm, however, the majority range from coarse silt to very fine sand. The calcareous beds have about less than 15% quartz grains and about 85% calcite; volume % of quartz and calcite was estimated using the comparison chart of Terry and Chillingar (1955).

5. Discussion

Carbonates occur as beds, lenses and concretions in the 2nd cycle of the Manndrapselva Member (upper Ediacaran) of the Stáhpogieddi Formation on the Digermulen Peninsula, Arctic Norway (Fig. 1a, b). To date, it has been thought that the entire upper Ediacaran and Cambrian succession of the area comprises only siliciclastic sedimentary rocks, which is not the case, as shown here. Previously, Banks (1973) reported on very thin beds composed of more than 50% ferroan calcite from the Indreelva Member. He considered the origin of the carbonate enigmatic, suggesting either derivation from calcareous microorganism or diagenetic alteration of terrigenous material. Because of the age of the succession, the former option is unlikely.

The occurrence of carbonates coincides with the absence of trace fossils in the section (Fig. 2). This could indicate that oxygen levels were too low for benthic life, or that another limiting factor such as salinity has become dominant making the environment unfavourable for macro-organisms. The absence of trace fossils may also be due to a combination of less favourable outcrop and erosion of the top layers of the sea bed soon after deposition, as flute casts occur on the bottom of some sandstone beds.

The studied sedimentary rocks contain framboidal pyrite. Pyrite-forming processes range from biogenetically induced to abiogenetic. Pyrite can form (1) in the depositional environment syngeneticaly by precipitation from an euxinic water column, (2) during diagenesis within the porewaters of anoxic sediments with overlying oxic/dysoxic water column, or (3) under mixed conditions where overlying water column shifts ephemerally between dysoxic and euxinic (Wilkin and Barnes, 1996; Bond and Wignall, 2010; Wang et al., 2012). The framboidal texture results from rapid nucleation in environments where iron monosulfide and pyrite are strongly supersaturated (e.g., Wilkin and Barnes, 1996; Butler and Pickard, 2000). Their formation during the earliest stages of anoxic diagenesis occurs within the bacterial sulphate reduction zone extending from about a few cm to 10 m depth below the sediment–water interface in marine environments (e.g., Curtis, 1977; Zimmerle, 1995; Wilkin et al., 1996). Sulphate and iron reduction by bacteria during decay processes of organic matter under anoxic conditions lead to pyrite formation at very shallow depths. The presence of pyrite in the studied sediments proves the chemically reducing conditions during their formation. Though the measurements here are limited, the size of the pyrite framboids (~10 μm on average, e.g. Fig. 8f) may suggest they formed within the porewaters of the sediment during early diagenesis (e.g., Wilkin et al. 1996; Bond and Wignall, 2010).

Sediments comprising carbonate concretions with spherulites that pass into a layer of CIC calcite are described from different depositional environments (e.g., Hodgson, 1968; Colquhoun, 1999). Those described by Hodgson (1968), were deposited presumably in deeper offshore environment (Hopgood, 1961) and those described by Colquhoun (1999) were deposited in deltaic/estuarine environment.

Based on the sedimentology and fossil record above and below the carbonate-bearing succession, the carbonates (mudstones and wackestones) forming individual beds in the 2nd cycle of the Manndrapselva Member precipitated in a marine depositional setting. On average the calcite spherulites discussed here are larger in diameter than those from other Precambrian occurrences (cf. Tucker, 1983; Seong-Joo and Golubic, 1999). For example, they resemble those from the Lower Cretaceous lacustrine carbonate reservoirs in the South Atlantic in regard to their size and appearance in the sediment (cf. Terra et al., 2010, fig. 21c; Wright and Barnett, 2015, pp. 212–213). Because of later compaction and tectono-thermal overprint, we can only speculate whether they formed under similar conditions as those described by Wright and Barnett (2015) and Herlinger et al. (2017) for the carbonate spherulites from the Lower Cretaceous lacustrine carbonate reservoirs. Considering the required conditions for the formation of carbonate spherulites, i.e. high alkaline conditions (e.g., Mercedes-Martín et al., 2017; Rogerson et al., 2017), we suggest two conceptual models for their formation (Fig. 9).

Model 1 suggests carbonate spherulite formation in a coastal littoral zone and later recycling and hydrodynamic transport into the marine sublittoral zone of the 2nd cycle of the Manndrapselva Member. Evidence for that, such as possible erosional features on spherulite grains, is however not recognizable due to later compaction and tectono-thermal overprint.

Model 2 suggests in situ formation of carbonate spherulites in the sublittoral zone, at the sediment–water interface at the seabed or a few cm below the interface. The temporarily required alkaline conditions may have been caused by upwelling of high alkalinity deep waters.

In both models, microbial communities may have been involved in the uptake of CO_2 from the water column which triggered precipitation of calcite nuclei, supported by the occurrence of extracellular polymeric substances, followed by fibro-radial growth of spherulites. As carbonate sediments may undergo pervasive changes during diagenesis, the depositional characteristics may be lost. It can be speculated that the spherulites were originally composed of vaterite or aragonite during initial crystallization. Because of the unstable nature of these calcium carbonate polymorphs, the initial mineralogy was replaced by calcite during early diagenesis, although, calcite may also be original (Tucker, 2001; Kirkham and Tucker, 2018). Whether original or replaced, the radial fibrous crystals of spherulites in calcareous concretions from the 2nd cycle of the Manndrapselva Member are currently calcite.

The porosity in mudrocks is reduced from 70–90% near the seabed where muds are deposited to about 30% at depths around 1–2 km mainly by compaction during diagenesis (Burst, 1969; Curtis, 1977; Tucker, 2001). The thickness of the sediment is reduced and much of the pore fluid is expelled. Further burial and compaction through increasing overburden together with increasing temperatures leads to further water loss together with changes in clay mineralogy. During the early stages of burial compaction, pore pressure increases by following the hydrostatic pressure gradient, as pore spaces are freely interconnected to the water table. During later stages, fluid is trapped as permeability declines and pore pressure increases to near lithostatic pressures. Because of the low permeability fluid pressure increases. Carbonate compaction is much more complicated, as cementation and dissolution processes either reduce or enhance the porosity during diagenesis. During burial diagenesis the loose spherulite grains became closely packed and fluid was trapped in intergranular pore space which was reduced by compaction and eventually cemented. The spherulite-bearing layers acted as preferred nucleation sites during the formation of whole concretions (Fig. 9d, e). Their cementation could have taken place anytime during their diagenesis.

Concretions are thought to form early in diagenesis. It is recognized at the outcrop that the bedding planes pass through the concretions, as clearly visible in Figure 4a, b. Inside some of the concretions, the bedding looks slightly deformed. Furthermore, the gentle deflection of bedding planes in the host rock around some of the concretions is still visible despite the overprinting pervasive cleavage (Figs. 4b and 5d). These field observations support that the concretions formed early in diagenesis after deposition of the sediments and probably continued to grow further during compaction.

Progressive concretionary growth stages of various distinct concretions have been distinguished throughout diagenesis (e.g., Raiswell, 1971; Sellés-Martínez, 1996). Raiswell (1971) suggested that CIC structures start growing in sediments with 30–40% porosity. The sediments must have been in a partly compacted state for calcite to nucleate on the surfaces of concretions (Woodland, 1964; Franks, 1969; Raiswell, 1971). Otherwise calcite would grow homogeneously throughout a watery sediment. Previous studies suggested that layer parallel fibrous veins, and CIC structures form by hydraulic fracturing due to fluid overpressure (e.g., Sellés-Martínez, 1994, 1996; Cosgrove, 2001; Sibson, 2003; Cobbold et al., 2013, and references therein). It was argued that fluid pressure must be high enough relative to overburden for fluid-filled fractures to form and fibres to grow perpendicular to the bedding. Formation of fractures is mainly controlled by the rock properties, stress state and pore-fluid pressure in the rock. It was suggested that orientation and spatial distribution of fractures and veins reflect the state of stress, thus also the boundary conditions in a basin (Cosgrove, 2001; Sibson, 2003, and references therein). Furthermore, it is generally accepted that calcite fibres grow in the direction of the opening of the veins. Thus, the orientation of CIC structures around the concretions and parallel to the bedding (with cone axes perpendicular to the bedding) indicate that the host sediments experienced a vertical dilation or a horizontal compression during their formation. Anisotropy in the succession with alternating horizontal beds of various lithologies leads to strength and permeability variations through the succession. Dilation can form along the weak interface between the relatively rigid calcareous concretions and the weak mudrocks and where fluid pressure is sufficiently high. According to Sibson (2017), in compressional regimes, sub-horizontal extension veins may develop over vertical intervals <1 km or so below low-permeability sealing horizons with rock tensile strengths about 10 to 20 MPa. Sub-horizontal extension veins may also develop at a deeper level where low-angle thrusting occurs (Sibson, 2017).

If the typical temperatures for CIC calcite formation are 70 °C to 120 °C (Criss et al., 1988; Cobbold et al., 2013), and assuming a 'normal' continental geothermal gradient of 25–30 °C (Allen and Allen, 2005), this temperature range corresponds to depths of approximately 2.3–4.8 km. Taking into account the sediment thickness of the overlying uppermost Ediacaran and lower Palaeozoic strata (Reading, 1965; Banks et al., 1971), CIC calcite formation (Fig. 9f, g) could have taken place at the earliest during the late Cambrian–Ordovician. The upper age limit for the formation of the concretions containing CIC calcite can be constrained as follows. A detailed view on one of the calcareous concretions reveals that the concretion formed post-sedimentary as the bedding passes through it (Fig. 4b). A low-angle cleavage cuts both the bedding and the concretion containing CIC calcite. Thus, presumably the concretion formed during the latest Ediacaran to Cambrian burial and diagenesis and clearly in pre-Caledonian time before deformation and metamorphism. The formation of CIC structures around the concretions and calcareous beds might be related to the very early onset of Caledonian tectonics (e.g., nappe thrusting toward the Baltica margin, maybe a far-field effect) as the CIC structures were cut at a small angle by the Caledonian cleavage, which provides the upper time limit for the CIC formation. Also, the Trollfjorden–Komagelva Fault Zone to the north of the study area (Fig. 1a) may have played a role during the formation of the CIC structures. The main activity along this fault zone has likely occurred during the Timanian orogeny in late Neoproterozoic and during the Caledonian orogeny in Silurian–Devonian times (e.g., Herrevold et al., 2009). Hence, whether the CIC formation is related to the activity along the Trollfjorden–Komagelva Fault Zone or onset of Caledonian deformation, or part of some intervening event, remains unclear. Currently, we do not have other constraints than those discussed above on the formation age of the CIC calcite. Further work will be necessary to fully constrain the timing of CIC calcite formation.

The high-angle veins (Figs. 4b and 5c) exist only inside the concretions and are not visible in the surrounding host rock. It seems like lithology had a control on where they occur. Furthermore, the veins cut the layering inside the concretion, for example the vein at the centre of the concretion in Figure 4b. Therefore, fractures formed and opened within the more competent concretions at significant depth after lithification under high fluid pressure conditions (Fig. 9f, g).

The succession was later deformed and metamorphosed during the Caledonian orogeny, which led to the pressure solution and pervasive cleavage cutting the bedding in the rocks (Figs. 4b, d, 5c, d and 9h). The high-angle calcite veins inside the concretions became slightly curved; some of the CIC calcite gained elongate to sigmoidal shape.

The calcite spherulites surrounded by a pore fluid were dissolved at the contact points where the differential stress was high and the dissolved material precipitated where the differential stress was low (Fig. 8). The clay-filled pressure solution seams and stylolites lie at a relatively low angle to the horizontal bedding and the dilation sites, consisting of the newly grown fibrous calcite along spherulite rims, are at a high angle to the bedding (Fig. 8c–e). The orientation of the overprinting pressure solution seams and calcite fibre growth agrees with the compaction induced by the Caledonian tectonic event.

Metamorphism was very low grade so that most of the (primary and secondary) sedimentary features are well preserved. This is also confirmed by the colour of the organic-walled microfossils, which suggests a post-mature level, indicating a thermal overprint of 200 to 250 °C (T. Palacios, unpublished data). The timing of deformation and metamorphic overprint including the cleavage formation can be assigned to the Caledonian orogeny (Meinhold et al., in press).

6. Conclusions

The discovery of carbonates in the upper Ediacaran succession (2nd cycle of the Manndrapselva Member) of northern Norway provides new insights into the palaeoenvironment and post-depositional processes at the western margin of Baltica during the late Precambrian and early Palaeozoic. Our study shows that:

i. Carbonates, some made up of calcite spherulites, formed locally under high alkaline conditions during the late Ediacaran.

ii. Calcareous concretions formed around spherulite-bearing lenses early in diagenesis after deposition of the sediments and probably continued to grow further during compaction.
iii. After reduction of porosity cone-in-cone (CIC) calcite was growing preferentially at overpressured horizons along the interface between the carbonates and surrounding siliciclastic sediments, probably during late Cambrian–Ordovician but clearly in pre-Caledonian time prior to metamorphism.
iv. The sedimentary succession was later deformed and metamorphosed during the Caledonian orogeny, which led to the pressure solution and pervasive cleavage cutting the bedding at a small angle.

In summary, in the late Ediacaran, temporary deposition of carbonates within the otherwise siliciclastic-dominated facies at the western edge of Baltica occurred. The upper Ediacaran carbonates have only been found in a limited area on the Digermulen Peninsula. However, it can be speculated that there might be prominent occurrences in other sections onshore or offshore Norway, waiting to be discovered. The new record of carbonates with calcite spherulites and CIC structures from the Ediacaran of Arctic Norway adds to their rare occurrences in the geological record.

Acknowledgements

In the framework of the Digermulen Early Life Research Group financial support for fieldwork in Arctic Norway and sample analysis was provided by the Research Council of Norway (Grant No. 231103). Sören Jensen and Teodoro Palacios acknowledge funding from Spanish "Ministerio de Economía, Industria y Competitividad" (Grant No. CGL 2017–87631-P). We are grateful to Adam Jeffery and Burkhard Schmidt for providing access to the SEM/EDX and μ-XRF facility respectively, and to Eugen Grădinaru for information on the cone-in-cone structures of Ukraine and Moldavia. This paper benefited from careful reviews by Alex Brasier and Steve Kershaw.

Appendix A. Supplementary data

Supplementary data associated with this article can be found, in the online version, at https://doi.org/xxxxx

References

Allen, P.A., Allen, J.R., 2005. Basin analysis: principles and applications, second ed. Blackwell Science Ltd, Oxford.

Allen, V.T., 1936. A mineralized spherulitic limestone in the Cheltenham fireclay. American Mineralogist 21, 369–373.

Banks, N.L., 1973. Innerelv Member: late Precambrian marine shelf deposit, east Finnmark. Norges Geologiske Undersøkelse 288, 7–25.

Banks, N.L., Edwards, M.B., Geddes, W.P., Hobday, D.K., Reading, H.G., 1971. Late Precambrian and Cambro-Ordovician sedimentation in East Finnmark. Norges Geologiske Undersøkelse 269, 197–236.

Bond, D.P.G., Wignall, P.B., 2010. Pyrite framboid study of marine Permian–Triassic boundary sections: A complex anoxic event and its relationships to contemporaneous mass extinction. Geological Society of America Bulletin 122, 1265–1279.

Buczynski, C., Chafetz, H.S., 1991. Habit of bacterially induced precipitates of calcium carbonate and the influence of medium viscosity on mineralogy. Journal of Sedimentary Petrology 61, 226–233.

Burst, J.F., 1969. Diagenesis of Gulf Coast clayey sediments and its possible relation to petroleum migration. American Association of Petroleum Geologists Bulletin 53, 73–93.

Butler, I.B., Pickard, D., 2000. Framboidal pyrite formation via oxidation of iron (II) monosulfide by hydrogen sulphide. Geochimica et Cosmochimica Acta 64, 2665–2672.

Cao, M., Zhong, J., Liu, C., Sun, N., Song, G., He, X., 2017. Features and genetic mechanism of cone-in-cone structures: Progress and examples. Journal of Palaeogeography 19, 1049–1062 (in Chinese).

Chafetz, H.S., Butler, J.C., 1980. Petrology of recent caliche pisolites, spherulites, and speleothem deposits from central Texas. Sedimentology 27, 497–518.

Chafetz, H., Barth, J., Cook, M., Guo, X., Zhou, J., 2018. Origins of carbonate spherulites: Implications for Brazilian Aptian pre-salt reservoir. Sedimentary Geology 365, 21–33.

Cobbold, P.R., Rodriguez, N., 2007. Seepage forces, important factors in the formation of horizontal hydraulic fractures and bedding-parallel fibrous veins (‘beef’ and ‘cone-in-cone’). Geofluids 7, 313–322.

Cobbold, P.R., Zanella, A., Rodrigues, N., Løseth, H., 2013. Bedding-parallel fibrous veins (beef and cone-in-cone): Worldwide occurrence and possible significance in terms of fluid overpressure, hydrocarbon generation and mineralization. Marine and Petroleum Geology 43, 1–20.

Colquhoun, I.M., 1999. On the origin of the calcite-cemented sandstones in the Clearwater Formation oil-sands, Alberta. PhD thesis, University of Western Ontario.

Cosgrove, J.W., 2001. Hydraulic fracturing during the formation and deformation of a basin: A factor in the dewatering of low-permeability sediments. American Association of Petroleum Geologists Bulletin 85, 737–748.

Criss, R.E., Cooke, G.A., Day, S.D., 1988. An origin for the carbonate concretions of the Ohio shale. U.S. Geological Survey Bulletin 1836, 1–21.

Curtis, C.D., 1977. Sediment geochemistry: Environments and processes dominated by involvement of an aqueous phase. In: Horne, J.E.T., Dunham, K. (Eds.), Mineralogy: Towards the Twenty-first Century. Philosophical Transactions of the Royal Society of London Series A, 286, pp. 353–372.

Dunham, R.J., 1962. Classification of carbonate rocks according to depositional texture. In: Ham, W.E. (Ed.), Classification of Carbonate Rocks. American Association of Petroleum Geologists Memoir, 1, pp. 108–121.

Fairchild, I.J., 1991. Origins of carbonate in Neoproterozoic stromatolites and the identification of modern analogues. Precambrian Research 53, 281–299.

Farmer, J., Vidal, G., Moczydłowska, M., Strauss, H., Ahlberg, P., Siedlecka, A., 1992. Ediacaran fossils from the Innerelv Member (late Proterozoic) of the Tanafjorden area, northeastern Finnmark. Geological Magazine 129, 181–195.

Franks, P.C., 1969. Nature, origin, and significance of cone-in-cone structures in the Kiowa Formation (Early Cretaceous), north-central Kansas. Journal of Sedimentary Petrology 39, 1438–1454.

Grotzinger, J.P., Kasting, J.F., 1993. New constraints on Precambrian ocean composition. Journal of Geology 101, 235–243.

Herlinger, R. Jr., Zambonato, E.E., De Ros, L.F., 2017. Influence of diagenesis on the quality of Lower Cretaceous Pre-salt lacustrine carbonate reservoirs from northern Campos Basin, offshore Brazil. Journal of Sedimentary Research 87, 1285–1313.

Herrevold, T., Gabrielsen, R.H., Roberts, D., 2009. Structural geology of the southeastern part of the Trollfjorden-Komagelva Fault Zone, Varanger Peninsula, Finnmark, North Norway. Norwegian Journal of Geology 89, 305–325.

Hodgson, W.A., 1968. The diagenesis of spherulitic carbonate concretions and other rocks from Mangakahia Group sediments, Kaipara Harbour, New Zealand. Journal of Sedimentary Petrology 38, 1254–1263.

Högström, A.E.S., Jensen, S., Palacios, T., Ebbestad, J.O.R., 2013. New information on the Ediacaran–Cambrian transition in the Vestertana Group, Finnmark, northern Norway, from trace fossils and organic-walled microfossils. Norwegian Journal of Geology 93, 95–106.

Högström, A.E.S., Ebbestad, J.O.R., Jensen, S., Palacios, T., Meinhold, G., Taylor, W.L., Novis, L.K., Agić, H., Moczydłowska, M., 2014. New occurrences and extension of the stratigraphical range of discoidal Ediacara-type fossils on the Digermul Peninsula, northern Norway. 58th Palaeontological Association Annual Meeting, Programme Abstracts, p. 75.

Högström, A.E.S., Jensen, S., Ebbestad, J.O.R., Taylor, W.L., Høyberget, M., Agić, H., Meinhold, G., Palacios, T., 2017. Expanding the Ediacaran biota on the Digermulen Peninsula, Arctic Norway. In: McIlroy, D. (Ed.), International Symposium on the Ediacaran–Cambrian transition 2017. Abstract Volume, p. 45.

Hooker, J.N., Cartwright, J., 2016. Dolomite overgrowths suggest a primary origin of cone-in-cone. Geological Magazine 155, 568–585.

Hopgood, A.M., 1961. The geology of the Cape Rodney–Kawau district, Auckland. New Zealand Journal of Geology and Geophysics 4, 205–230.

Ivantsov, A.Y., Gritsenko, V.P., Paliy, V.M., Velikanov, V.A., Konstantinenko, L.I., Menasova, A.S., Fedonkin, M.A., Zakrevskaya, M.A., Serezhnikova, E.A., 2015. Upper Vendian macrofossils of Eastern Europe, Middle Dniester area and Volhynia. PIN RAS, Moscow, 144 pp. (in Russian)

Jensen, S., Högström, A.E.S., Høyberget, M., Meinhold, G., Palacios, T., Taylor, W.L., Ebbestad, J.O.R., Agić, H., 2017. Trace fossils across the Ediacaran-Cambrian boundary on the Digermulen Peninsula, Arctic Norway. In: McIlroy, D. (Ed.), International Symposium on the Ediacaran–Cambrian transition 2017, Abstract Volume, p. 48.

Jensen, S., Högström, A.S., Almond, J., Taylor, W.L., Meinhold, G., Høyberget, M., Ebbestad, J.O.R., Agić, H., Palacios, T., 2018a. Scratch circles from the Ediacaran and Cambrian of Arctic Norway and the Republic of South Africa, with a review of scratch circle occurrences. Bulletin of Geosciences 93, 287–304.

Jensen, S., Högström, A.E.S., Høyberget, M., Meinhold, G., McIlroy, D., Ebbestad, J.O.R., Taylor, W.L., Agić, H., Palacios, T., 2018b. New occurrences of *Palaeopascichnus* from the Stáhpogieddi Formation, Arctic Norway, and their bearing on the age of the Varanger Ice Age. Canadian Journal of Earth Sciences 55, 1253–1261.

Kershaw, S., Guo, L., 2016. Beef and cone-in-cone calcite fibrous cements associated with the end-Permian and end-Triassic mass extinctions: Reassessment of processes of formation. Journal of Palaeogeography 5, 28–42.

Kirkham, A., Tucker, M.E., 2018. Thrombolites, spherulites and fibrous crusts (Holkerian, Purbeckian, Aptian): Context, fabrics and origins. Sedimentary Geology 374, 69–84.

Kolokol'tsev, V.G., 2002. The cone-in-cone structure and its origin. Lithology and Mineral Resources 37, 523–535.

Kopeliovich, A.V., 1965. Epigenez drevnikh tolshch yugo-zapada russkoj platformy. Akademiya Nauk SSSR Geologicheskij Institut, Trudy 121. Nauka, Moscow.

Kowal-Linka, M., 2010. Origin of cone-in-cone calcite veins during calcitization of dolomites and their subsequent diagenesis: A case study from the Gogolin Formation (Middle Triassic), SW Poland. Sedimentary Geology 224, 54–64.

McBride, E.F., Picard, M.D., Milliken, K.L., 2003. Calcite-cemented concretions in Cretaceous sandstone, Wyoming and Utah, U.S.A. Journal of Sedimentary Research 73, 462–483.

McIlroy, D., Brasier, M.D., 2017. Ichnological evidence for the Cambrian explosion in the Ediacaran to Cambrian succession of Tanafjord, Finnmark, northern Norway. In: Brasier, A.T., McIlroy D., McLoughlin, N. (Eds.), Earth System Evolution and Early Life: a Celebration of the Work of Martin Brasier. Geological Society, London, Special Publication, 488, pp. 351–368.

Meinhold, G., Wemmer, K., Högström, A.E.S., Ebbestad, J.O.R., Jensen, S., Palacios, T., Høyberget, M., Agić, H., Taylor, W.L., in press. A late Caledonian tectono-thermal event in the Gaissa Nappe Complex, Arctic Norway: evidence from fine-fraction K–Ar dating and illite crystallinity from the Digermulen Peninsula. GFF. https://doi.org/10.1080/11035897.2019.1583685.

Meert, J.G., 2014. Ediacaran–Ordovician paleomagnetism of Baltica: A review. Gondwana Research 25, 159–169.

Mercedes-Martín, R., Rogerson, M.R., Brasier, A.T., Vonhof, H., Prior, P.J., Fellows, S.M., Reijmer, J.J.G., Billing, I., Pedley, H.M., 2016. Growing spherulitic calcite grains in saline, hyperalkaline lakes: experimental evaluation of the effects of Mg–clays and organic acids. Sedimentary Geology 335, 93–102.

Mercedes-Martín, R., Brasier, A.T., Rogerson, M., Reijmer, J.J.G., Vonhof, H., Pedley, M., 2017. A depositional model for spherulitic carbonates associated with alkaline volcanic lakes. Marine and Petroleum Geology 86, 168–191.

Nesterovsky, V.A., Chupryna, A.M., Ruzina, M.V., Soldatenko, Y.V., Albani, A.E., 2017. Stratigraphic levels of Vendian (Ediacaran) black shales of the Transdniestrian Podillia. Scientific Bulletin of National Mining University 3, 12–19.

Parnell, J., Blamey, N.J.F., Costanzo, A., Feely, M., Boyce, A.J., 2014. Preservation of Mesoproterozoic age deep burial fluid signatures, NW Scotland. Marine and Petroleum Geology 55, 275–281.

Pettijohn, F.J., 1975. Sedimentary Rocks, third ed. Harper International Edition, Harper & Row, Publishers Inc., New York.

Raiswell, R., 1971. The growth of Cambrian and Liassic concretions. Sedimentology 17, 147–171.

Reading, H.G., 1965. Eocambrian and Lower Palaeozoic geology of the Digermul Peninsula, Tanafjord, Finnmark. Norges Geologiske Undersøkelse 234, 167–191.

Rice, A.H.N., 2014. Restoration of the external Caledonides, Finnmark, North Norway. In: Corfu, F., Gasser, D., Chew, D.M. (Eds.), New Perspectives on the Caledonides of Scandinavia and related areas. Geological Society of London, Special Publications, 390, pp. 271–299.

Riding, R., 2008. Abiogenic, microbial and hybrid authigenic carbonate crusts: components of Precambrian stromatolites. Geologica Croatica 61, 73–103.

Rogerson, M., Mercedes-Martín, R., Brasier, A.T., Mcgill, R.A.R., Prior, T.J., Vonhof, H., Fellows, S.M., Reijmer, J.J.G., McClymont, E., Billing, I., Matthews, A., Pedley, H.M., 2017. Are spherulitic lacustrine carbonates an expression of large-scale mineral carbonation? A case study from the East Kirkton Limestone, Scotland. Gondwana Research 48, 101–109.

Saller, A., Rushton, S., Buambua, L., Inman, K., McNeil, R., Dickson, J.A.D., 2016. Presalt stratigraphy and depositional systems in the Kwanza Basin, offshore Angola. American Association of Petroleum Geologists Bulletin 100, 1135–1164.

Sellés-Martínez, J., 1994. New insights in the origin of cone-in-cone structures. Carbonates and Evaporites 9, 172–186.

Sellés-Martínez, J., 1996. Concretion morphology, classification and genesis. Earth-Science Reviews 41, 177–210.

Seong-Joo, L., Golubic, S., 1999. Microfossil populations in the context of synsedimentary micrite deposition and acicular carbonate precipitation: Mesoproterozoic Gaoyuzhuang Formation, China. Precambrian Research 96, 183–208.

Sibson, R.H., 2003. Brittle failure controls on maximum sustainable overpressure in different tectonic regimes. American Association of Petroleum Geologists Bulletin 87, 901–908.

Sibson, R.H., 2017. Tensile overpressure compartments on low-angle thrust faults. Earth, Planets and Space 69, article number 113, doi:10.1186/s40623-017-0699-y

Siedlecka, A., Reading, H.G., Williams, G.D., Roberts, D., 2006. Langfjorden, preliminary bedrock geology map 2236 II, scale 1:50.000. Norges Geologiske Undersøkelse, Trondheim.

Smith, M.D., 2009. Stratigraphic and geochemical evolution of the Old Fort Point Formation, southern Canadian Cordillera: The deep-marine perspective of Ediacaran post-glacial environmental change. PhD thesis, University of Ottawa, Ottawa, 430 pp.

Tarr, W.A., 1932. Cone-in-cone. In: Twenhofel, W.H. (Ed.), Treatise on Sedimentation. Williams & Wilkins, Baltimore, pp. 716–733.

Terra, G.J.S., Spadini, A.R., França, A.B., Sombro, C.L., Zambonato, E.E., da Silva Juschaks, L.C., Arienti, L.M., Erthal, M.M., Blauth, M., Franco, M.P., Matsuda, N.S., da Silva, N.G.C., Moretti, P.A., D'Avila, R.S.F., de Souza, R.S., Tonietto, S.N., dos Anjos, S.M.C., Campinho, V.S., Winter, W.R., 2010. Classificação de rochas carbonáticas aplicável às bacias sedimentares brasileiras. Boletin Geociencias Petrobras 18, 9–29.

Terry, R.D., Chillingar, G.V., 1955. Summary of "Concerning some additional aids in studying sedimentary formations" by M. S. Shvetsov. Journal of Sedimentary Petrology 25, 229–234.

Tucker, M.E., 1983. Sedimentation of organic-rich limestones in the Late Precambrian of southern Norway. Precambrian Research 22, 295–315.

Tucker, M.E., 2001. Sedimentary petrology, third ed. Blackwell Science Ltd, Oxford.

Turner, E.C., Kamber, B.S., 2012. Arctic Bay Formation, Borden Basin, Nunavut (Canada): basin evolution, black shale, and dissolved metal systematics in the Mesoproterozoic ocean. Precambrian Research 208–211, 1–18.

Usdowski, H.-E., 1963. Die Genese der Tutenmergel oder Nagelkalke (cone-in-cone). Beiträge zur Mineralogie und Petrographie 9, 95–110.

Văscăutanu, T., 1931. Les formations siluriennes de la rive Roumaine du Dneister. Anuarul Institutului Geologic al României 15, 425–663.

Verrecchia, E.P., Freyyet, P., Verrecchia, K.E., Dumont, J.-L., 1995. Spherulites in calcrete laminar crusts: Biogenic $CaCO_3$, Precipitation as a major contributor to crust formation. Journal of Sedimentary Research A65, 690–700.

Wang, L., Shi, X., Jiang, G., 2012. Pyrite morphology and redox fluctuations recorded in the Ediacaran Doushantuo Formation. Palaeogeography, Palaeoclimatology, Palaeoecology 333, 218–227.

Wilkin, R.T., Barnes, H.L., 1996. Pyrite formation by reactions of iron monosulfides with dissolved inorganic and organic sulfur species. Geochemica et Cosmochemica Acta 60, 4167–4179.

Wilkin, R.T., Barnes, H.L., Brantley, S.L., 1996. The size distribution of framboidal pyrite in modern sediments: An indicator of redox conditions. Geochemica et Cosmochemica Acta 60, 3897–3912.

Woodland, B.G., 1964. The nature and origin of cone-in-cone structure. Fieldiana: Geology 13, 185–305.

Wright, V.P., Barnett, A.J., 2015. An abiotic model for the development of textures in some South Atlantic early Cretaceous lacustrine carbonates. In: Bosence, D.W., Gibbons, K.A., Le Heron, D.P., Morgen W.A., Pritchard, T., Vining, B.A., (Eds.), Microbial Carbonates in Space and Time: Implications for Global Exploration and Production. Geological Society of London, Special Publications, 418, pp. 209–219.

Xiao, S., Knoll, A.H., Kaufman, A.J., Yin, L., Zhang, Y., 1997. Neoproterozoic fossils in Mesoproterozoic rocks? Chemostratigraphic resolution of a biostratigraphic conundrum from the North China Platform. Precambrian Research 84, 197–220.

Zimmerle, W., 1995. Petroleum sedimentology. Ferdinand Enke, Stuttgart.

Figure captions

Figure 1. (a) Outline of northernmost Scandinavia showing the Vestertana Group rocks, in grey shade, preserved within the Gaissa Nappe Complex (GNC) and para-autochthonous in eastern Finnmark on the Varanger Peninsula (VP). Red box marks study area. TKFZ – Trollfjorden–Komagelva Fault Zone. **(b)** Simplified stratigraphy of the Vestertana Group (after Jensen et al., 2018b), showing occurrences of carbonates and cone-in-cone calcite first described in this study. **(c)** Geology of the south-east portion of the Digermulen Peninsula, based on Siedlecka et al. (2006), showing locality where carbonates – some with calcite spherulites and cone-in-cone calcite – were found within the Manndrapselva Member. **(d)** Late Ediacaran (550 Ma) palaeogeographic reconstruction of Baltica (after Meert, 2014). Land (ochre) and shallow sea (light blue) distributions were adopted from the palaeogeographic map series of Ron Blakey (Colorado Plateau Geosystems, http://cpgeosystems.com/). Red star marks study area.

Figure 2. Log of the 2nd cycle of the Manndrapselva Member of the Digermulen Peninsula, Finnmark, Arctic Norway. The stratigraphic occurrence of trace fossils, the problematica *Harlaniella* and *Palaeopascichnus delicatus*, and carbonates is shown. Carbonate beds, lenses and concretions are all shown as blue ellipsoids for simplicity.

Figure 3. Schematic illustrations of calcite spherulite and cone-in-cone (CIC) structures.

Figure 4. Upper Ediacaran sedimentary rocks from the 2nd cycle of the Manndrapselva Member of the Digermulen Peninsula, Finnmark, Arctic Norway. **(a)** Turbiditic succession containing calcareous beds, lenses and concretions (ochre colour) with CIC calcite. **(b)** Detailed view of calcareous concretion shown in **(a)**. The continuation of the bedding within the concretion is well visible along the central part. A high angle calcite vein within the concretion cuts the bedding. Thin veins and cracks at the centre and lower right have similar geometry with slightly curved shape and tip splays. A low-angle cleavage cuts both the bedding and the concretion. **(c)** Turbiditic succession containing calcareous beds (below hammer) with CIC calcite. **(d)** Detailed view of part of Fig. 4c showing CIC calcite, indicated by white arrow. **(e)** Concretion with an outer CIC calcite layer, a relatively coarse calcareous

granular middle layer containing calcite spherulites and a calcareous siliciclastic central layer. **(f)** CIC calcite with the cone apices pointing upwards towards the concretion. The base of the closely packed cones is aligned parallel to the bedding with the mudstones.

Figure 5. (a, b) Top-surface views showing weathering features of calcareous lenses and concretions with CIC calcite. Circular shape of the cone bases on the surface creates positive **(a)**, neutral **(b)** relief depending on the intensity of weathering. **(c)** Vertical section of the concretion. The cone apices of the CIC calcite around the concretion rim point towards the concretion. Note two calcite veins at the centre of the concretion. **(d)** Caledonian cleavage cuts the concretion and bedding in the host rock. The bedding in the host rock bend around the concretion close to its margins (indicated by triangular arrows). The concretion has a slightly sigmoidal shape with its left and right margins parallel to the pervasive cleavage in the host rock. The CIC calcite along the upper part of the concretion is cut by the pervasive cleavage and disturbed. However, the cone shape of the CIC calcite is still recognized (indicated by white arrows) along the left margin and below the concretion. Note the change in rock colour, cleavage intensity (i.e. pervasive with millimetre to centimetre spacing in the mudstones and siltstones and much wider in the calcareous concretion) and cleavage refraction along different bedding planes.

Figure 6. (a, b) Cut and polished hand specimens show the layered nature of the calcareous concretions. Samples D16-G81 and D17-GM4 correspond to the specimens TSGF 18430 and TSGF 18431, respectively, catalogued in the geological collections of the Arctic University Museum of Norway. **(c, d)** Colour-inverted images of vertical sections in **(a, b)** highlight the layered subdivision. The outer layer (top and bottom) consists of nested cones of fibrous calcite (CIC structures). The inner layers show thinly laminated calcareous siliciclastics and carbonate spherulites. **(e, f)** Selection of μ-XRF elemental maps illustrate very well the subdivision into various layers. Additional μ-XRF elemental maps are provided as Supplementary data (see Appendix A). All images oriented with top up.

Figure 7. Thin-section photomicrographs. All images oriented with top up. The TSGF numbers given below refer to the corresponding thin sections catalogued in the geological collections of the Arctic University Museum of Norway. **(a)** CIC structures with well

preserved conic geometry (sample D16-G81, TSGF 18432), in plane light. The cone axes are vertical. The large cones are made up of attached smaller cones. The cone faces are irregularly corrugated and lined by clay minerals. Some of the cones are truncated by and partly dissolved along the low-angle cleavage planes (indicated by white arrows). Pressure solution seams, consisting of mainly dark clay minerals and oxides, extend from upper left to lower right along with the cleavage planes. **(b)** CIC calcite (sample D17-GM4, TSGF 18433), in plane light. The small conical bundles are visible on the larger cones. **(c, d)** CIC calcite cut by the cleavage (sample D17-GM4, TSGF 18433), in crossed nicols. The cleavage extends from upper left to lower right at a low angle. CIC calcite is visible in domains less affected by the deformation between the cleavage planes. Calcite fibres show partial extinction. Cone apices in **(a–d)** point towards the calcareous concretions. **(e)** Calcareous siliciclastic bed (sample D17-GM5, TSGF 18434), in crossed nicols. Angular quartz grains (white and grey spots) float in a calcite matrix. **(f)** Close-up view of **(e)**. Quartz grain size ranges from coarse silt to very fine sand.

Figure 8. Thin-section photomicrographs **(a–e)**. All images oriented with top up. The TSGF numbers given below refer to the corresponding thin sections catalogued in the geological collections at the Arctic University Museum of Norway. **(a, b)** Calcite spherulites and calcareous siliciclastic layer transition (sample D17-GM4, TSGF 18433), in crossed nicols. The layering is horizontal. Dark, thin pressure solution seams are oblique to the bedding. Note the half calcite spherulite in **(b)** along the contact with calcareous siliciclastic layer. **(c)** Layer of calcite spherulites (sample D17-GM4, TSGF 18433), in crossed nicols. Calcite spherulites show well developed radial extinction. Note the partial dissolution along the contact zone of two relatively large calcite spherulites between which stylolites are developed, at the central lower left of the image. **(d)** Calcite spherulites (sample D16-G81, TSGF 18432), in plane light. Pressure solution seams and stylolite extend from upper left to lower right. Extensional fissures are oriented at a high angle to bedding some with newly grown calcite fibres. **(e)** Close-up view, in plane light. The new calcite fibre grew alongside the spherulites. The dark central part contains mainly clay minerals and oxides. **(f)** Backscattered electron image of pyrite framboids (sample D17-GM4, TSGF 18433). Inset shows a close-up.

Figure 9. Conceptional models of the depositional environment and the development of carbonate spherulites, concretions, and CIC structures in the 2nd cycle of the Manndrapselva Member (upper Ediacaran) through time. Numbers (1) and (2) in Figure 9a refer to the two models discussed in Section 5. Model 1 suggests carbonate spherulite formation in a coastal littoral zone and later recycling and hydrodynamic transport into the marine sublittoral zone. Evidence for that such as possible erosional features on spherulite grains is however lacking due to later compaction and tectono-thermal overprint. For simplification, Model 1 is therefore not shown in detail here. Model 2 suggests in situ formation of carbonate spherulites in the sublittoral zone, at the sediment–water interface at the seabed or a few cm below the interface.

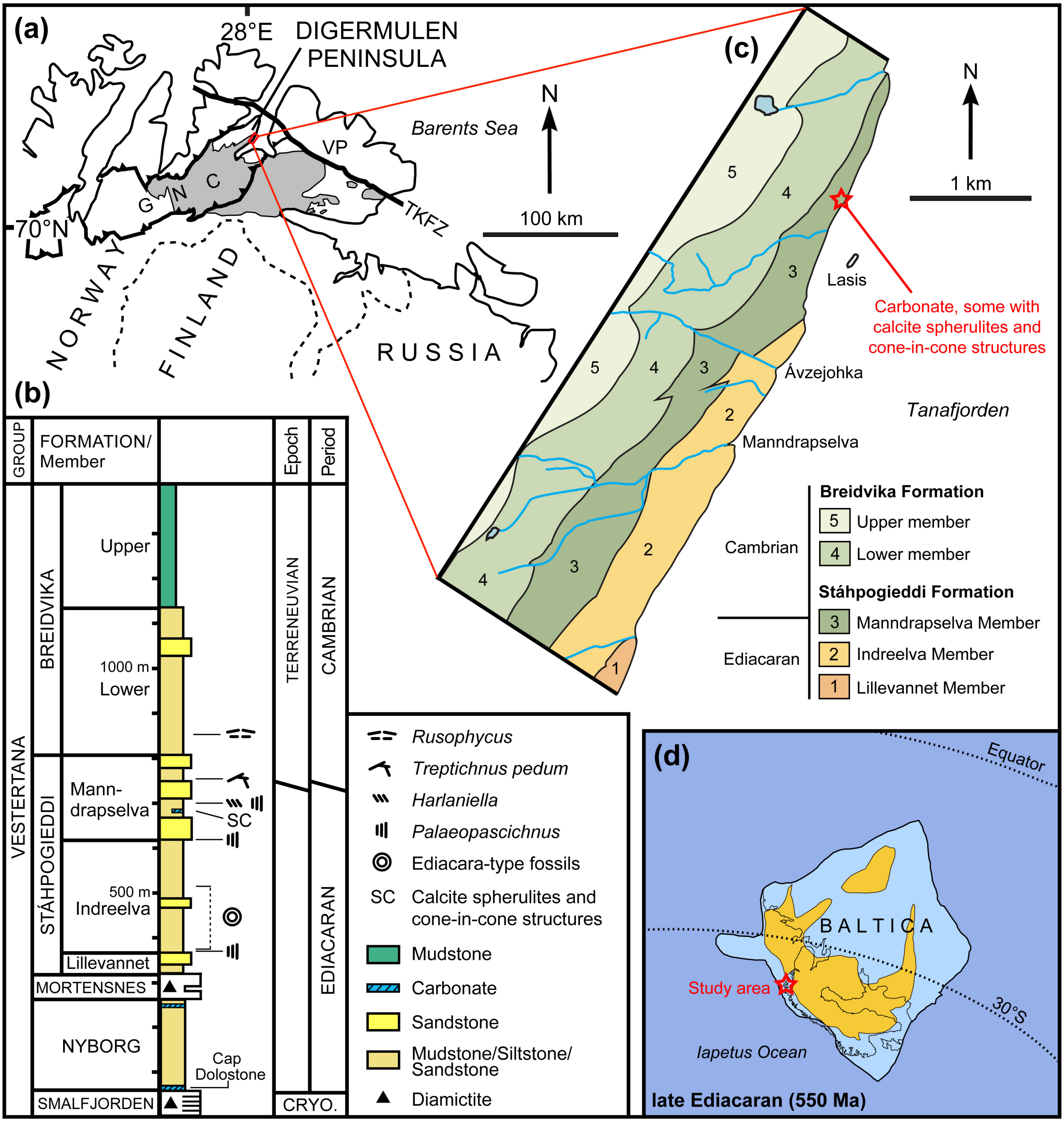
(a)
28°E
DIGERMULEN PENINSULA
Barents Sea
VP
G
N
C
TKFZ
70°N
100 km
NORWAY
FINLAND
RUSSIA
(b)
GROUP
FORMATION/ Member
Epoch
Period
VESTERTANA
BREIDVIKA
Upper
1000 m
Lower
STÁHPOGIEDDI
Mann-drapselva
SC
500 m
Indreelva
Lillevannet
MORTENSNES
NYBORG
Cap Dolostone
SMALFJORDEN
TERRENEUVIAN
CAMBRIAN
EDIACARAN
CRYO.
Rusophycus
Treptichnus pedum
Harlaniella
Palaeopascichnus
Ediacara-type fossils
SC Calcite spherulites and cone-in-cone structures
Mudstone
Carbonate
Sandstone
Mudstone/Siltstone/ Sandstone
Diamictite
(c)
N
1 km
Lasis
Carbonate, some with calcite spherulites and cone-in-cone structures
Ávzejohka
Tanafjorden
Manndrapselva
Breidvika Formation
5 Upper member
4 Lower member
Cambrian
Stáhpogieddi Formation
3 Manndrapselva Member
2 Indreelva Member
1 Lillevannet Member
Ediacaran
(d)
Equator
BALTICA
Study area
30°S
Iapetus Ocean
late Ediacaran (550 Ma)

Figure 1

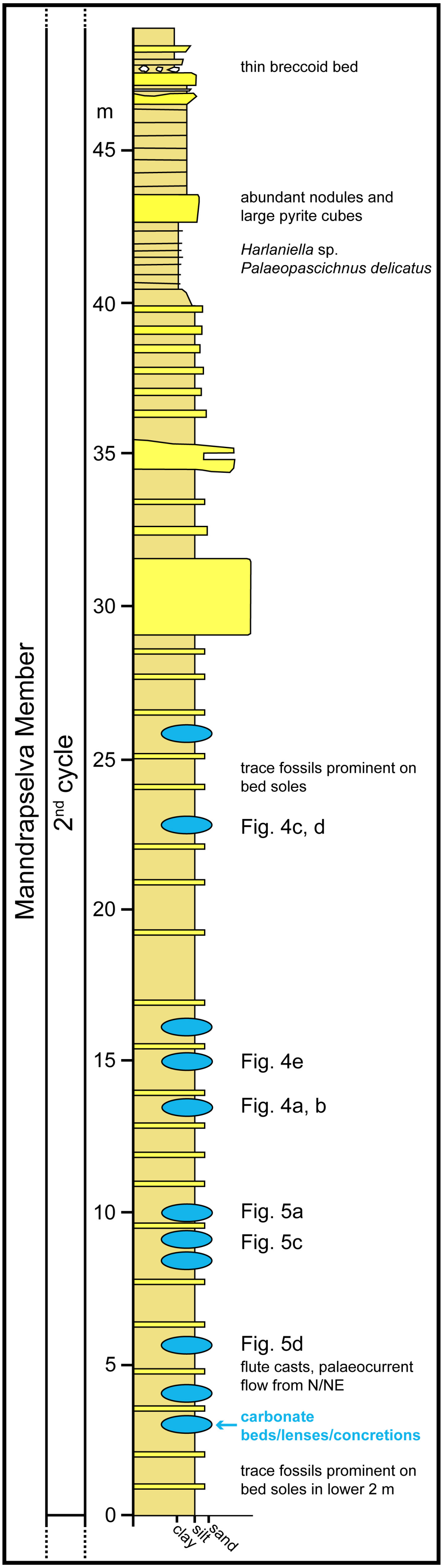

Manndrapselva Member
2nd cycle
m
45
40
35
30
25
20
15
10
5
0
clay
silt
sand
thin breccoid bed
abundant nodules and
large pyrite cubes
Harlaniella sp.
Palaeopascichnus delicatus
trace fossils prominent on
bed soles
Fig. 4c, d
Fig. 4e
Fig. 4a, b
Fig. 5a
Fig. 5c
Fig. 5d
flute casts, palaeocurrent
flow from N/NE
carbonate
beds/lenses/concretions
trace fossils prominent on
bed soles in lower 2 m

Figure 2

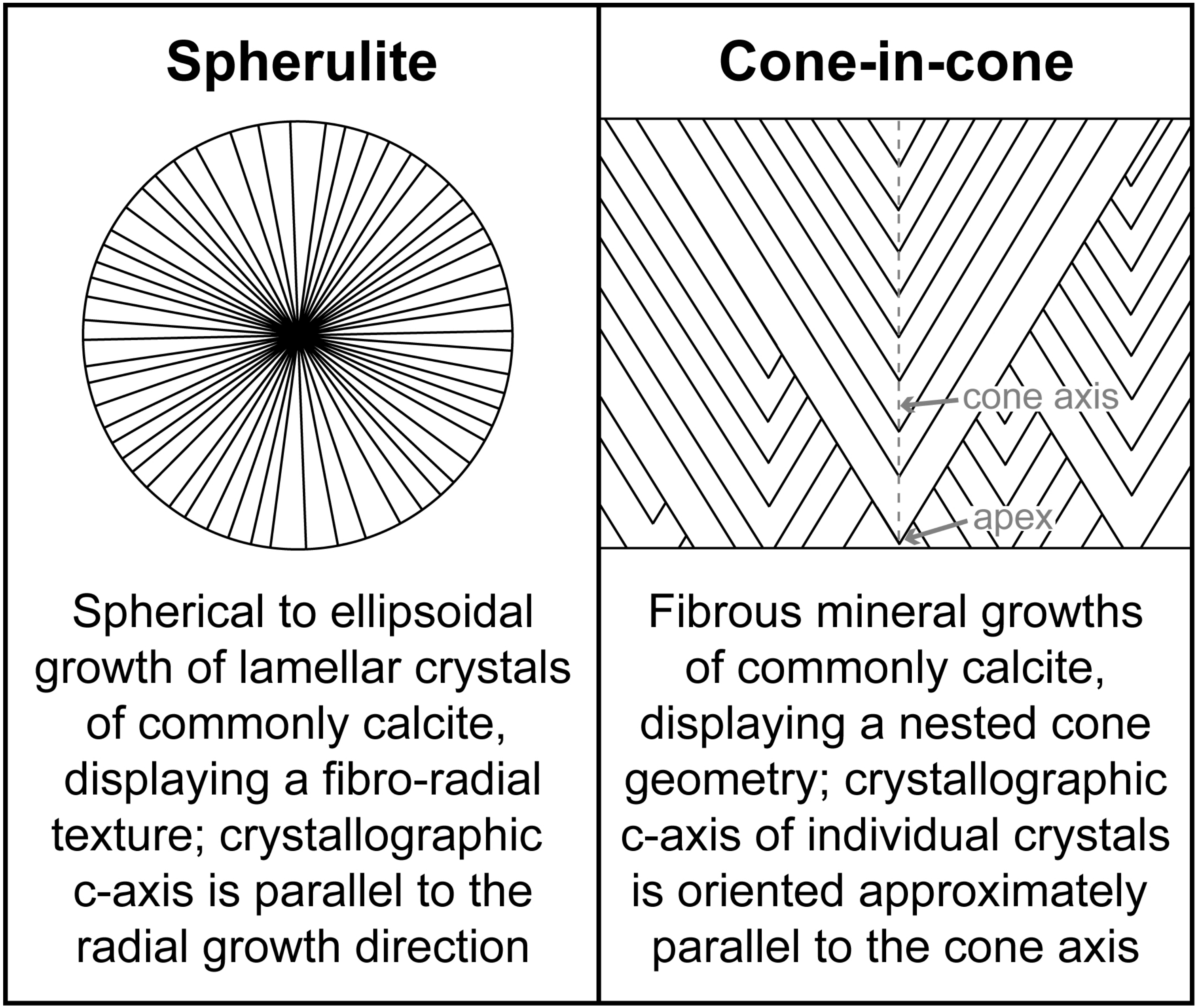
Spherulite
Cone-in-cone
cone axis
apex
Spherical to ellipsoidal growth of lamellar crystals of commonly calcite, displaying a fibro-radial texture; crystallographic c-axis is parallel to the radial growth direction
Fibrous mineral growths of commonly calcite, displaying a nested cone geometry; crystallographic c-axis of individual crystals is oriented approximately parallel to the cone axis

Figure 3


(a)
Digermulen
(b)
Early Life Research Group
CIC
(c)
Fig. 4d
(d)
CIC
(e)
spherulites
CIC
~2 cm
(f)
~1 cm

Figure 4

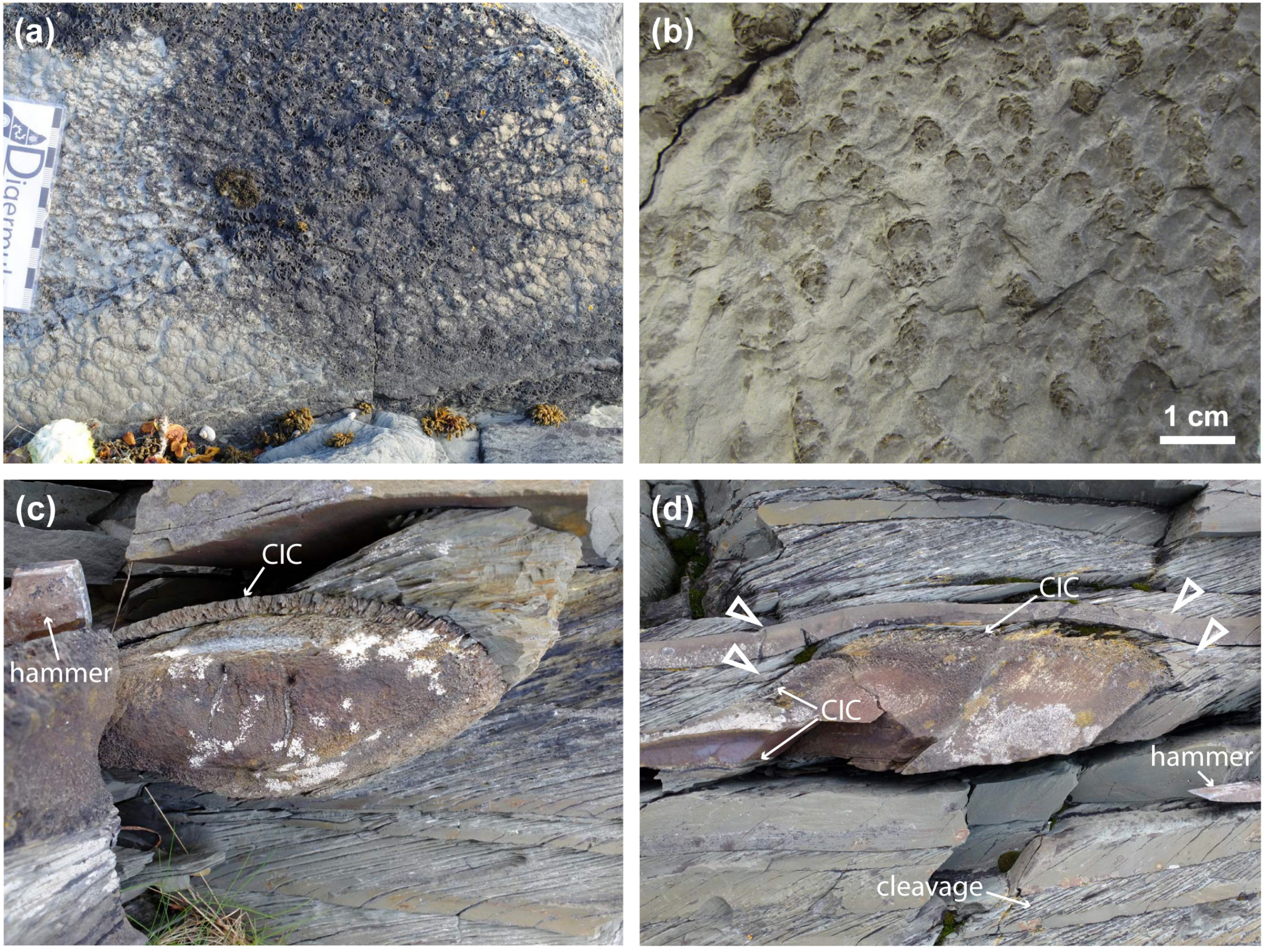

Figure 5

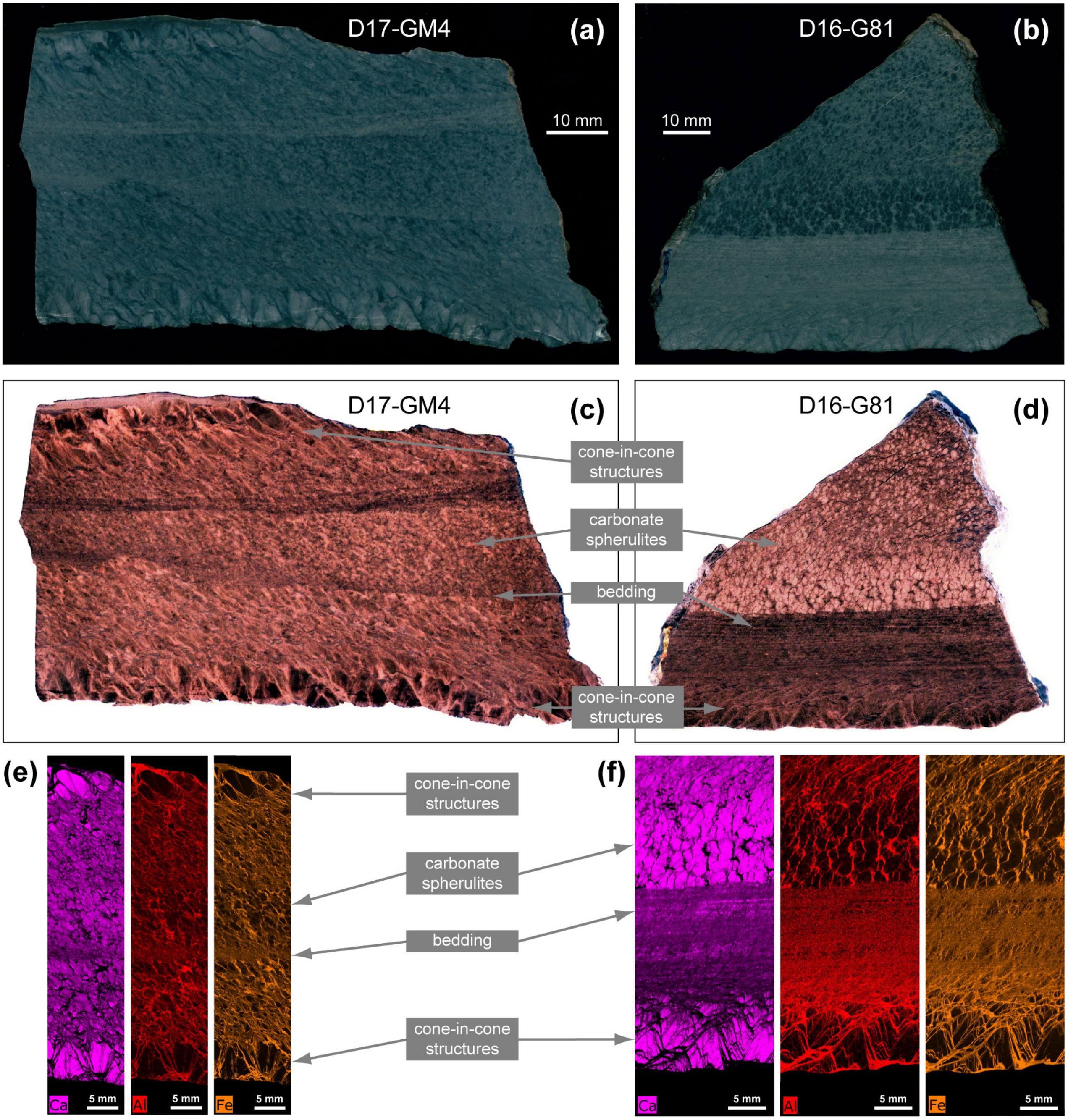

D17-GM4
(a)
10 mm
D16-G81
(b)
10 mm
D17-GM4
(c)
D16-G81
(d)
cone-in-cone structures
carbonate spherulites
bedding
cone-in-cone structures
(e)
(f)
cone-in-cone structures
carbonate spherulites
bedding
cone-in-cone structures
Ca
5 mm
Al
5 mm
Fe
5 mm
Ca
5 mm
Al
5 mm
Fe
5 mm

Figure 6

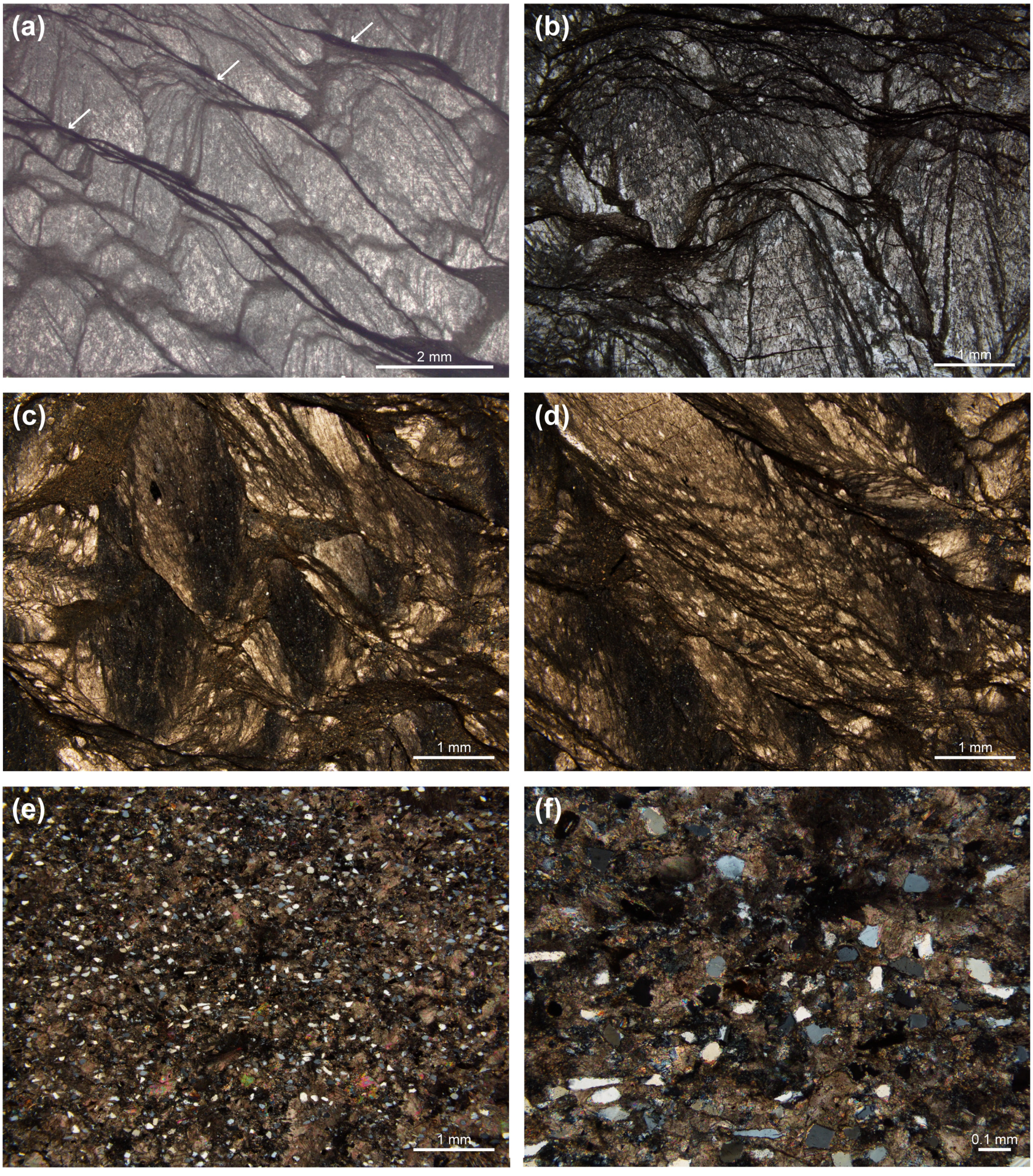

Figure 7

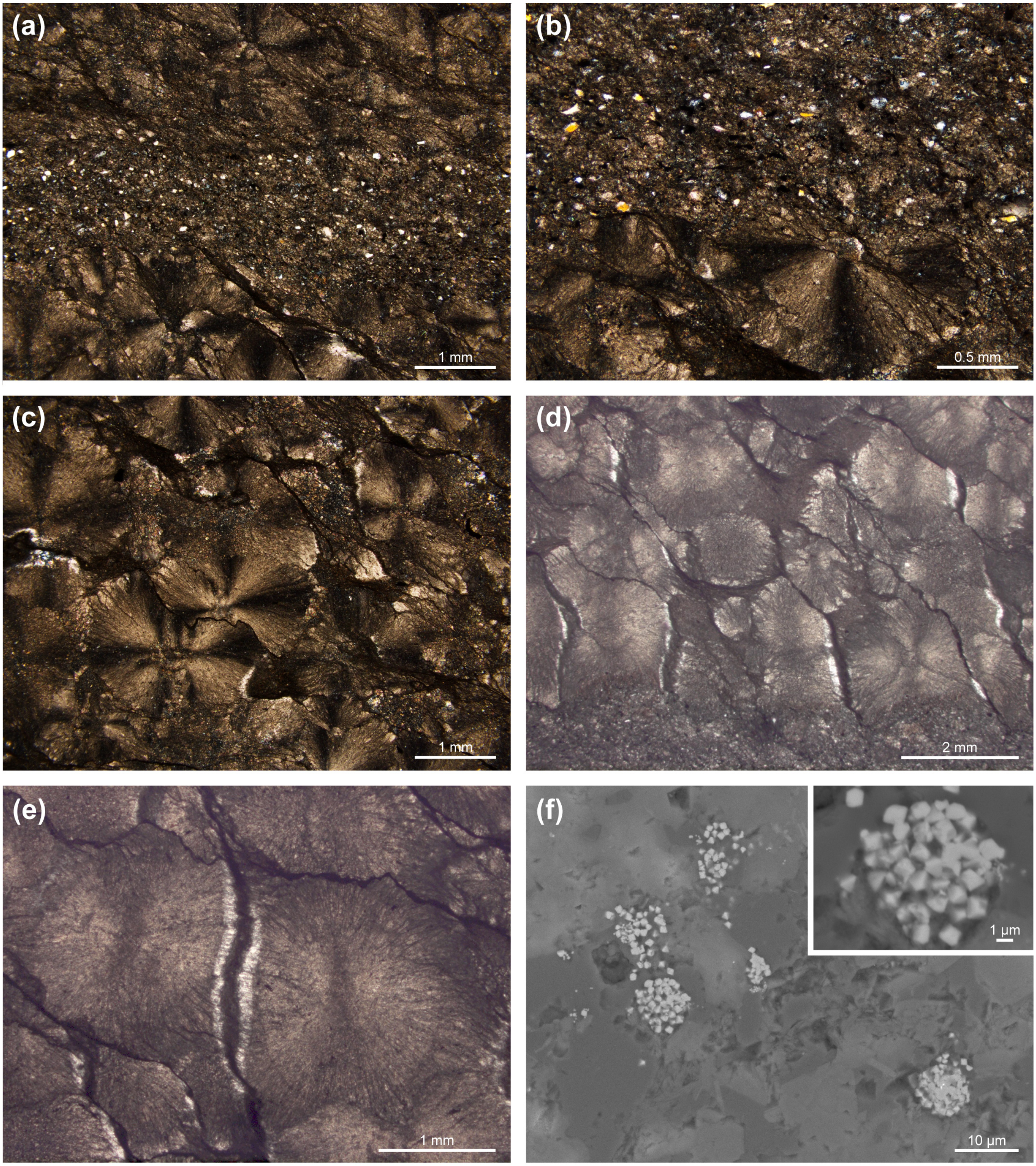

Figure 8

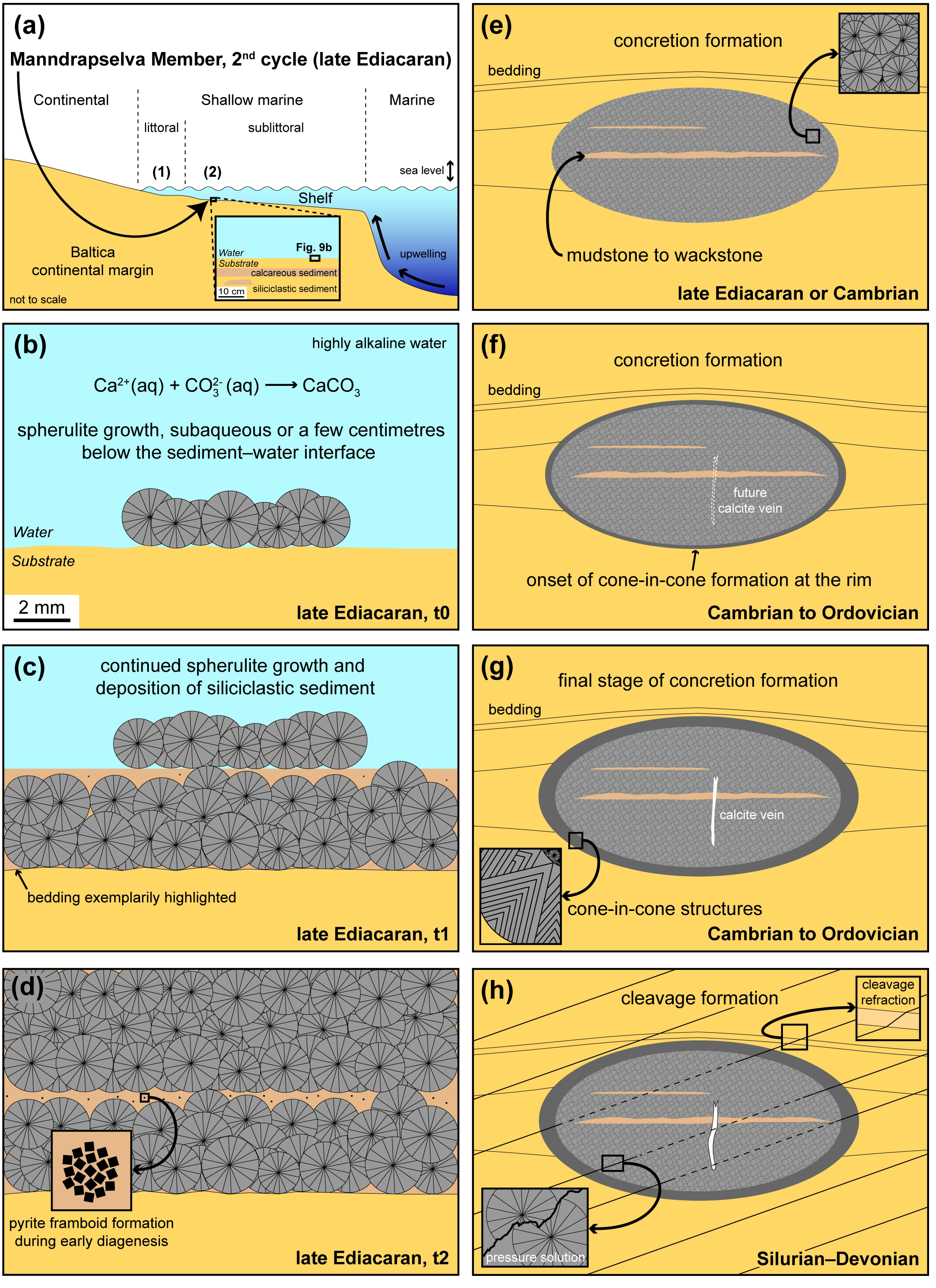

(a)
Manndrapselva Member, 2nd cycle (late Ediacaran)
Continental
Shallow marine
Marine
littoral
sublittoral
(1)
(2)
sea level
Shelf
Water
Substrate
Fig. 9b
calcareous sediment
siliciclastic sediment
10 cm
upwelling
Baltica
continental margin
not to scale
(b)
highly alkaline water
$Ca^{2+}(aq) + CO_3^{2-}(aq) \longrightarrow CaCO_3$
spherulite growth, subaqueous or a few centimetres
below the sediment–water interface
Water
Substrate
2 mm
late Ediacaran, t0
(c)
continued spherulite growth and
deposition of siliciclastic sediment
bedding exemplarily highlighted
late Ediacaran, t1
(d)
pyrite framboid formation
during early diagenesis
late Ediacaran, t2
(e)
concretion formation
bedding
mudstone to wackstone
late Ediacaran or Cambrian
(f)
concretion formation
bedding
future
calcite vein
onset of cone-in-cone formation at the rim
Cambrian to Ordovician
(g)
final stage of concretion formation
bedding
calcite vein
cone-in-cone structures
Cambrian to Ordovician
(h)
cleavage formation
cleavage
refraction
pressure solution
Silurian–Devonian

Figure 9

Supplementary data

First record of carbonates with spherulites and cone-in-cone structures from the Precambrian of Arctic Norway, and their palaeoenvironmental significance

Guido Meinhold[1,2,*], Sören Jensen[3], Magne Høyberget[4], Arzu Arslan[5], Jan Ove R. Ebbestad[6], Anette E. S. Högström[7], Teodoro Palacios[3], Heda Agić[8], Wendy L. Taylor[9]

[1]*School of Geography, Geology and the Environment, Keele University, Keele, Staffordshire, ST5 5BG, UK*

[2]*Department of Sedimentology and Environmental Geology, University of Göttingen, Goldschmidtstraße 3, D-37077 Göttingen, Germany*

[3]*Área de Paleontología, Facultad de Ciencias, Universidad de Extremadura, Avenida de Física, E-06006 Badajoz, Spain*

[4]*Rennesveien 14, N-4513 Mandal, Norway*

[5]*Newcastle-under-Lyme, Staffordshire, ST5 2ND, UK*

[6]*Museum of Evolution, Uppsala University, Norbyvägen 16, SE 752 36 Uppsala, Sweden*

[7]*Arctic University Museum of Norway, UiT - The Arctic University of Norway, N-9037 Tromsø, Norway*

[8]*Department of Earth Science, University of California at Santa Barbara, Santa Barbara, CA 93106, USA*

[9]*Department of Geological Sciences, University of Cape Town, Private Bag X3, Rondebosch 7701, Republic of South Africa*

*Corresponding author.

E-mail address: g.meinhold@keele.ac.uk (G. Meinhold).

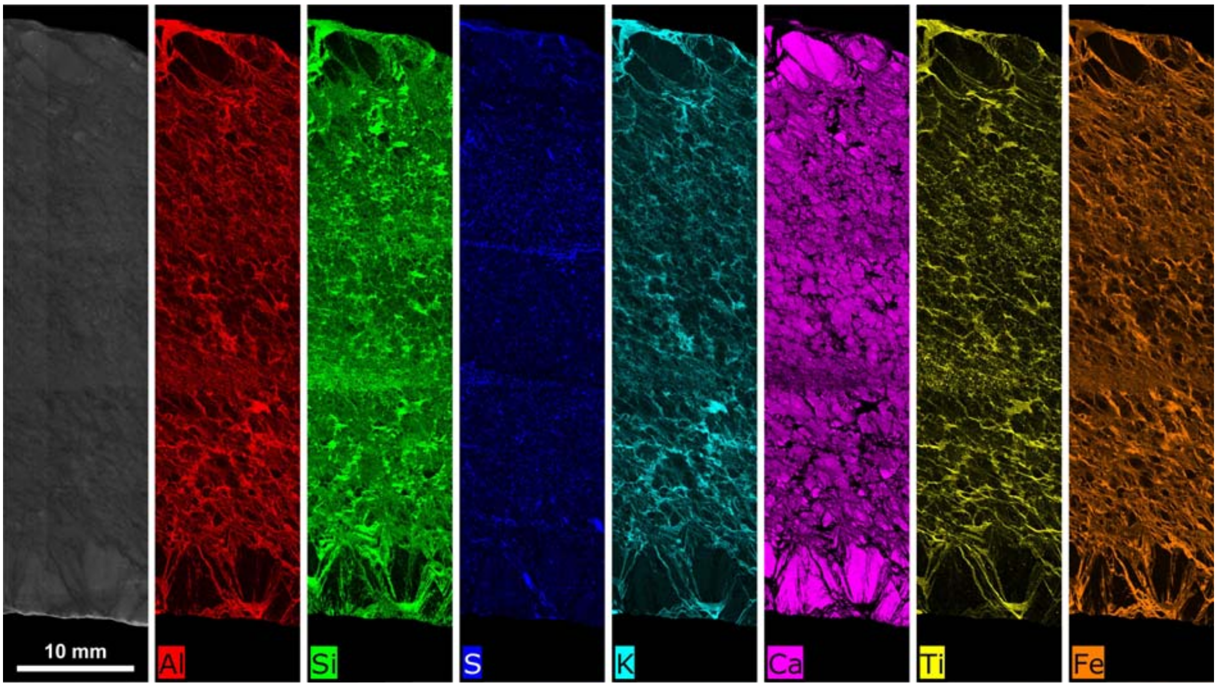

Figure S1. Vertical section of calcareous hand specimen (sample D17-GM4) from the 2nd cycle of the Manndrapselva Member containing cone-in-cone (CIC) structures chemically mapped with a μ-XRF spectrometer. The μ-XRF elemental maps (Al, Si, S, K, Ca, Ti, and Fe) illustrate very well the subdivision into various layers. The outer layer (top and bottom) consists of nested cones of fibrous calcite (CIC structures). The CIC structures along the top layer are more affected by the deformation. The inner layers show thinly laminated calcareous siliciclastics and carbonate spherulites. All images oriented with top up.

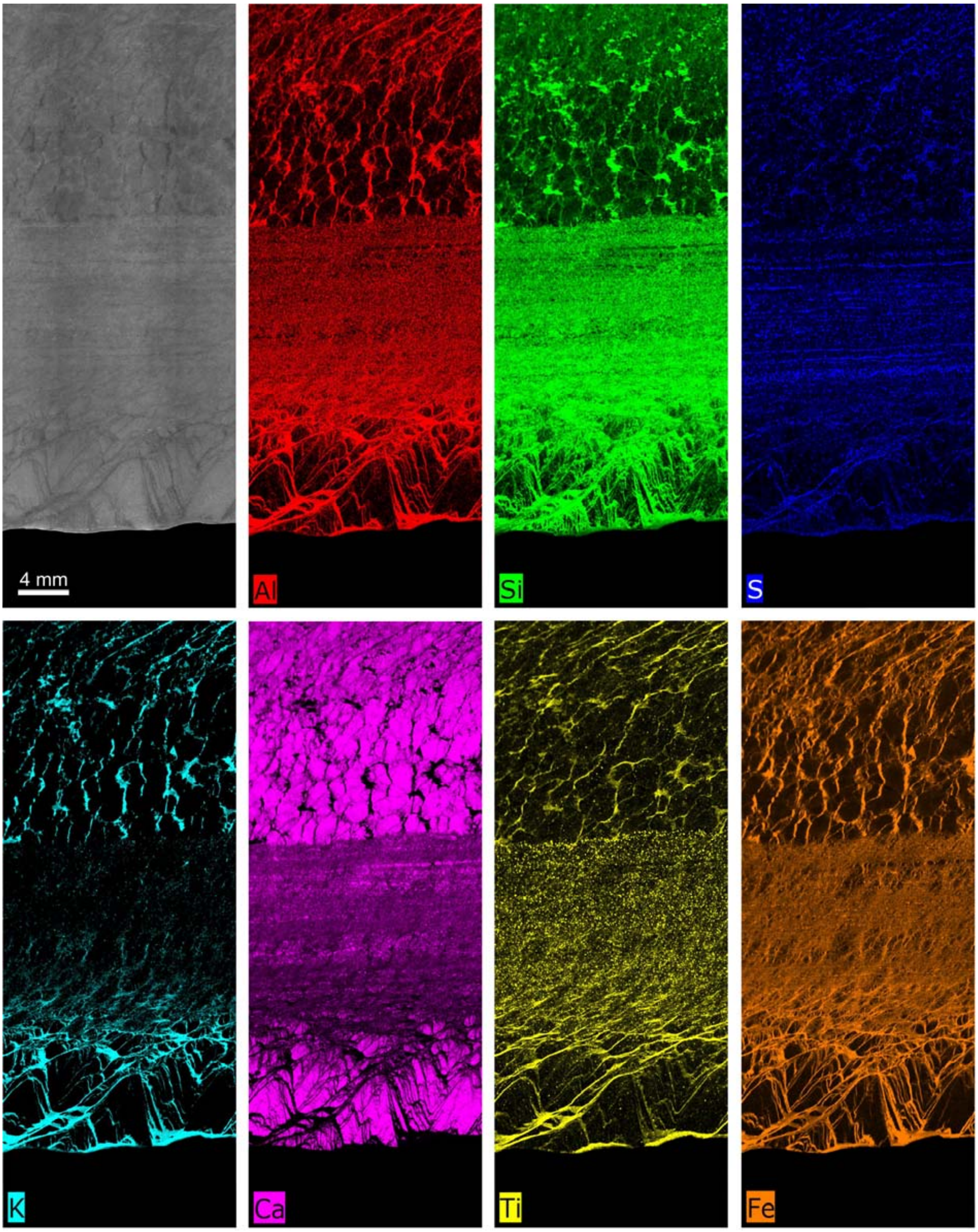

Figure S2. Vertical section of calcareous hand specimen (sample D16-G81) from the 2nd cycle of the Manndrapselva Member containing cone-in-cone (CIC) structures chemically mapped with a μ-XRF spectrometer. The μ-XRF elemental maps (Al, Si, S, K, Ca, Ti, and Fe) illustrate very well the subdivision into various layers. The outer layer (bottom) consists of nested cones of fibrous calcite (CIC structures). The middle layer is made up of thinly laminated calcareous siliciclastics, and the inner layer (top) of carbonate spherulites. All images oriented with top up.